Nematic polar anchoring strength measured by electric field techniques

Yu. A. Nastishin,[a] R. D. Polak, S. V. Shiyanovskii,[b] V. H. Bodnar,[c] and O. D. Lavrentovich[c,d]

Liquid Crystal Institute, Kent State University, Kent, Ohio 44242

We analyze the high-electric-field technique designed by Yokoyama and van Sprang [J. Appl. Phys. **57**, 4520 (1985)] to determine the polar anchoring coefficient W of a nematic liquid crystal-solid substrate. The technique implies simultaneous measurement of the optical phase retardation and capacitance as functions of the applied voltage well above the threshold of the Frederiks transition. We develop a generalized model that allows for the determination of W for tilted director orientation. Furthermore, the model results in a new high-field technique, (referred to as the RV technique), based on the measurement of retardation versus applied voltage. W is determined from a simple linear fit over a well-specified voltage window. No capacitance measurements are needed to determine W when the dielectric constants of the liquid crystal are known. We analyze the validity of the Yokoyama–van Sprang (YvS) and RV techniques and show that experimental data in real cells often do not follow the theoretical curves. The reason is that the director distribution is inhomogeneous in the plane of the bounding plates, while the theory assumes that the director is not distorted in this plane. This discrepancy can greatly modify the fitted value of $1/W$, and even change its sign, thus making the determination of W meaningless. We suggest a protocol that allows one to check if the cell can be used to measure W by the YvS or RV techniques. The protocol establishes new criteria that were absent in the original YvS procedure. The results are compared with other data on W, obtained by a threshold-field technique for the same nematic-substrate pair. © *1999 American Institute of Physics.* [S0021-8979(99)07020-6]

I. INTRODUCTION

The surface plays a dual role in liquid crystal physics. First, it constrains the liquid crystal and thus modifies the density and the surface scalar order parameter. Second, it orients the liquid crystal director. The equilibrium director orientation set by anisotropic molecular interactions at the surface in the absence of any external fields is called the "easy axis." An external field can deviate the director from the easy axis. Experimental determination of the work needed to reorient the director (represented by an "anchoring strength" or "anchoring coefficient") is of prime importance in understanding the surface phenomena in liquid crystals.[1–8] There are numerous techniques to achieve the goal. Testing techniques deduce anchoring strength from characterization of surface-stabilized wall defects,[2] distorted director in wedge cells,[3] or from light scattering at surface fluctuations.[4] External-field techniques measure director deviations as the function of the applied field.[5–21] The field techniques use dielectric or diamagnetic Frederiks effects in intermediate[5–10] or high fields,[11–16] as well as polar effects of flexoelectric[17] and surface polarization[18] origin. Each technique has its own limitations that often require specific ma-

terial parameters (e.g., sign of the dielectric anisotropy) or the direction of the easy axis. A more serious problem is that of reproducibility: analysis of the current literature makes it clear that anchoring strength data may differ by two to three orders of magnitude[1] when measured by different groups, even for the same pair of liquid crystal and substrate. We will show that the problem is not in the lack of diligence on the part of experimentalists, but rather in the intrinsic complexity of liquid crystal behavior at the substrate.

Especially difficult is the determination of the polar part of the anchoring energy that characterizes director deviations with respect to the normal to the surface. One of the reasons is that the polar anchoring often appears to be much stronger than the azimuthal (in-plane) anchoring and thus implies strong external torques (i.e., high voltages) to deviate the director from the easy axis. A reliable, simple, and reproducible protocol for polar anchoring strength measurement is still to be determined.

The most widely used technique[14] to determine the polar part W of the anchoring strength is that suggested by Yokoyama and van Sprang.[12] The Yokoyama–van Sprang (YvS) method is based on simultaneous measurement of capacitance C and optical phase retardation R as a function of the voltage V applied to the nematic cell. A very attractive feature of this technique is that in a certain range (V_{min}, V_{max}) of applied voltages, R is a linear function of the reciprocal electric displacement $(\sim 1/CV)$ and W (normalized by an elastic constant) can be simply deduced from the intercept of this linear dependence with the R axis. Unfortunately, the proper choice of the range (V_{min}, V_{max}) presents a problem.

4199   © 1999 American Institute of Physics

According to Ref. 12, the range (V_{min}, V_{max}) is determined by the following considerations. First, V_{min} should be well above the Frederiks threshold $[V_{min} \cong 6 V_{th}$ (Ref. 12)] to assure that the director in the middle of the cell is parallel to the field. This is why the method is often referred to as the 'high-electric-field' technique.[12] Second, the field-induced director deviations from the easy axis should be sufficiently small to justify expansion of the anchoring potential; this requirement limits V_{max}. As a result, the choice of V_{max} is ambiguous since V_{max} depends on W, and W is not known *a priori*. The problem can be addressed by comparing W's measured by YvS technique (preferably with different V_{max}'s, to W measured by an independent technique. Despite a bulk of research reports employing the YvS technique, we were unable to find such a comparative analysis. A related drawback is that the restrictions on the range (V_{min}, V_{max}) lead to a practical recipe to use thick cells, 40–60 μm or more.[12] Taken literally, this recipe of thick cells has been employed in all subsequent applications of the YvS technique. The circumstance is important: W might be thickness dependent in the presence of ions[19] but one is normally interested to know W in thin, say, 5 μm cells used in display applications. Finally, a serious problem seems to be that, as indicated by Yokoyama[20] and Ji *et al.*,[21] the YvS technique sometimes yields *negative* values of W. Stallinga *et al.*[22] observed an electrooptical response of cells that also points towards a negative value of W.

The goal of this article is to analyze the reliability of the YvS technique and the recently suggested RV technique.[16] The RV technique implies the measurement of optical phase retardation (but not the capacitance) as a function of applied voltage. We demonstrate that in many cases both techniques cannot provide meaningful values of the anchoring strength: the fit of experimental data can produce practically any value of W, including the negative ones, within the allowed fitting region (V_{min}, V_{max}). Analysis reveals that the experimental dependencies, such as R vs $1/CV$, measured for real cells, often do not follow the predictions of the theoretical model on which the YvS technique is based. One source of these discrepancies is that, in real cells, the director orientation and anchoring strength are not uniform in the plane of the cell, while the theory assumes strict uniformity. The problem is especially pronounced in cells with etched electrodes needed in the YvS technique. In contrast, the RV technique[16] does not require etched electrodes and significantly enhances the reliability of W measurements. Finally, this work also suggests a protocol that might be used to verify the validity of the obtained results.

The article is organized as follows.

Theoretical background is given in Sec. II. We consider a nematic cell with a tilted easy axis and calculate the relevant response characteristics (such as C and R) as the functions of the applied field, anchoring strength, etc. The Yokoyama–van Sprang formulas[12] are recovered as a specific case. This analysis predicts that the anchoring strength can be measured without separate measurements of capacitance and for relatively thin cells. Section III describes experimental techniques used to prepare the alignment layers and to assemble and characterize the cells. Section IV details
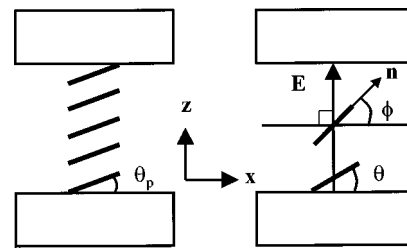

FIG. 1. Director configuration in the cell without field (left) and with an applied electric field (right).

measurements of W by the YvS technique and by the new RV technique. In many cases, W cannot be determined, since the cell does not behave in the way expected from the theory. For example, many cells show voltage-dependent excess retardation that does not reduce to such mundane factors as retardation of the alignment layers. Section V describes an independent attempt to estimate W for the same liquid crystal-substrate pairs. Section VI discusses possible causes of spurious results such as voltage-dependent and negative W; among these, nonuniformity of the surface parameters plays an important role. Finally, we propose a protocol that can be used to verify the very applicability of the YvS and RV techniques for a nematic cell prepared to measure W.

II. THEORETICAL BACKGROUND

A. Yokoyama–van Sprang technique

The goal is to determine the polar anchoring strength from the director response to the electric field. The problem boils down to the calculations of such characteristics as the capacitance and retardation of the cell as a function of the applied voltage. These functions have already been calculated for infinite strong anchoring.[23]

Consider a nematic liquid crystal confined between two identical electrodes located at $z=0$ and $z=d$ as shown in Fig. 1. In absence of the external fields, the director is oriented uniformly along the easy axis that makes an angle θ_p with respect to the x axis. The angle θ_p defines the minimum of the surface anchoring potential and is called the pretilt angle. In a sufficiently high electric field, there is a distortion of the liquid crystal director in the $x-z$ plane.

The free energy per unit area of the liquid crystal can be written as

$$F = \int_0^d f_b dz + f_s(0) + f_s(d), \tag{1}$$

where $f_b = \frac{1}{2}[(K_1 \cos^2 \phi + K_3 \sin^2 \phi)(d\phi/dz)^2 - \mathbf{D} \cdot \mathbf{E}]$ is the bulk free energy density, K_1 (K_3) is the splay (bend) elastic constant, $\mathbf{D} = \epsilon_0 \hat{\epsilon} \mathbf{E}$ is the electric displacement, $\hat{\epsilon}$ is the tensor of relative dielectric permittivity, $\mathbf{E}$ is the applied electric field (the applied voltage $V = \int_0^d E_z dz$), and ϕ is the angle between the director and the x axis. Assuming that deviation of the actual surface director orientation $\theta = \phi(0) = \phi(d)$ from θ_p is small, we use the Rapini–Papular approximation for the anchoring energy $f_s = \frac{1}{2} W \sin^2(\theta - \theta_p)$. Note that we neglect any possible effects of the divergence K_{13} term in f_b.

We assume that the effects of free electric charges are negligible, so that div $\mathbf{D}=0$, and, in a cell with a one-dimensional distortion, D_z does not depend on z:

$$D_z = \frac{\epsilon_0 V}{\int_0^d (\epsilon_\perp \cos^2 \phi + \epsilon_\parallel \sin^2 \phi)^{-1} dz}, \qquad (2)$$

where $\epsilon_\parallel$ and $\epsilon_\perp$ are the components of the dielectric tensor that are parallel and perpendicular to the director, respectively.

Because of symmetry about the cell midpoint, the Euler–Lagrange equation becomes

$$\left(\frac{d\phi}{dz}\right)^2$$
$$= \frac{\gamma D_z^2}{K_1 \epsilon_0 \epsilon_\perp} \frac{\sin^2 \phi_m - \sin^2 \phi}{(1+\kappa \sin^2 \phi)(1+\gamma \sin^2 \phi)(1+\gamma \sin^2 \phi_m)}, \qquad (3)$$

where $\gamma = (\epsilon_\parallel - \epsilon_\perp)/\epsilon_\perp$, $\kappa = (K_3 - K_1)/K_1$, and $\phi_m = \phi(d/2)$ is the maximum director angle. Solving Eq. (3) we obtain the applied voltage V, optical phase retardation R, and capacitance C as integral parametric functions with parameters $y_m = \sin^2 \phi_m$ and $y_b = \sin^2 \theta$:

$$V = \frac{V_{\text{th}}}{\pi} \sqrt{1+\gamma y_m} I_V(y_b, y_m), \qquad (4)$$

$$R = \frac{2\pi d n_0 \nu}{\lambda} \frac{I_R(y_b, y_m)}{I_C(y_b, y_m)}, \qquad (5)$$

$$C = \frac{\epsilon_0 \epsilon_\perp S}{d} \frac{I_C(y_b, y_m)}{I_V(y_b, y_m)}, \qquad (6)$$

where $V_{\text{th}} = \pi \sqrt{K_1/\epsilon_0 \epsilon_a}$, $\epsilon_a = \epsilon_\parallel - \epsilon_\perp$, $\nu = (n_e^2 - n_o^2)/n_e^2$, n_o and n_e are ordinary and extraordinary refractive indices, respectively, λ is the wavelength of the probing light, S is the overlapping electrode area, and

$$I_V(y_b, y_m) = \int_{y_b}^{y_m} \sqrt{\frac{(1+\kappa y)}{(1+\gamma y)(y_m - y)y(1-y)}} dy, \qquad (7)$$

$$I_R(y_b, y_m)$$
$$= \int_{y_b}^{y_m} \sqrt{\frac{(1+\kappa y)(1+\gamma y)(1-y)}{(y_m - y)y[1-\nu(1-y)]}} \frac{dy}{1+\sqrt{(1-\nu(1-y))}}, \qquad (8)$$

$$I_C(y_b, y_m) = \int_{y_b}^{y_m} \sqrt{\frac{(1+\kappa y)(1+\gamma y)}{(y_m - y)y(1-y)}} dy. \qquad (9)$$

The balance of torques at the boundary $[(\partial f_b/\partial \phi)/\partial z]_{z=0} = \partial f_s/\partial \theta$ gives the expression for the anchoring coefficient W

$$W = \frac{2K_1 I_C}{d \sin 2(\theta - \theta_p)} \sqrt{\frac{(1+\kappa y_b)(y_m - y_b)}{(1+\gamma y_b)}}. \qquad (10)$$

As one can see from Eqs. (4–9), there is one-to-one correspondence between pairs (y_m, y_b) and any two of (V, C, R). In other words, the pairs (V, R) or (V, C) completely describe the director configuration in the cell, and the

dependence $R(V)$ or $C(V)$ can be used to determine W for any pretilt angle. Moreover, it is not difficult to extend the consideration to the materials with $\epsilon_a < 0$.

Although W can be obtained by fitting the curve $R(V)$ without any other approximations, we also want to derive simplified formulas similar to that of YvS method. The approximation is based on asymptotic behavior of integrals (7)–(9) when $y_m \to 1$ and $y_b \to y_p = \sin^2 \theta_p$. The significant feature of these integrals is that I_V and I_C diverge logarithmically when $y_m \to 1$, whereas I_R does not. Noticing also, that for small deviations of boundary angle, all the integrals depend linearly on $s_b = \sin(\theta - \theta_p)$, one obtains the following approximate formulas:

$$I_{V,C}(y_b, y_m) = A_{V,C} t + P_{V,C}(y_p) - B_{V,C} s_b, \qquad (11a)$$

$$I_R(y_b, y_m) = I_R(y_p, 1) - B_R s_b, \qquad (11b)$$

where

$$t = -\ln(1-y_m); \quad A_V = \sqrt{\frac{1+\kappa}{1+\gamma}};$$

$$A_C = \sqrt{(1+\gamma)(1+\kappa)}; \quad B_V = 2\sqrt{\frac{1+\kappa y_p}{(1+\gamma y_p)(1-y_p)}};$$

$$B_C = 2\sqrt{\frac{(1+\kappa y_p)(1+\gamma y_p)}{1-y_p}};$$

$$B_R = \frac{2}{1+\sqrt{1-\nu(1-y_p)}} \sqrt{\frac{(1+\kappa y_p)(1+\gamma y_p)(1-y_p)}{1-\nu(1-y_p)}},$$

and $I_R(y_p, 1)$ and $P_{V,C}(y_p)$ are nonsingular parts of integrals that depend only on material constants of the studied LC and pretilt angle θ_p: $P_{V,C}(y_p) = \lim_{y_m \to 1}[I_{V,C}(y_p, y_m) + A_{V,C} \ln(1-y_m)]$.

Making a product from Eqs. (4), (5), and (6), we obtain an important formula for the further analysis of the YvS method, valid for any pretilt angle:

$$RCV = \frac{2\pi n_0 \nu \epsilon_0 \epsilon_\perp S}{\lambda} \sqrt{\frac{K_1}{\epsilon_0 \epsilon_a}} \sqrt{1+\gamma y_m} I_R(y_b, y_m). \qquad (12)$$

The main advantage of this expression is that when the approximation (11b) is valid, all changes in the RCV product are caused by director reorientation at the surface. For example, when the anchoring is infinitely strong, $W \to \infty$, then $RCV \to$ const. Since the surface changes are rather small, the first validity condition ($y_m \to 1$) for Eq. (11b), that provides constant bulk contribution, is very important. The inequality $V > V_{\min} = 6V_{\text{th}}$, originally suggested in the YvS method, satisfies this condition with extremely high accuracy ($1-y_m < 3 \times 10^{-6}$). The second condition, that the surface reorientation is small, is less crucial for determination of W and is determined mostly by the validity of substituting the actual anchoring profile with the Rapini–Papoular potential. Assuming that the Rapini–Papoular potential is valid when $s_b < 0.2$, we obtain the upper voltage limit

$$V_{\max} = \frac{0.2}{\pi \cos \theta_p} \sqrt{\frac{\epsilon_\perp}{\epsilon_\parallel}} \frac{Wd}{K_1} V_{\text{th}}.$$
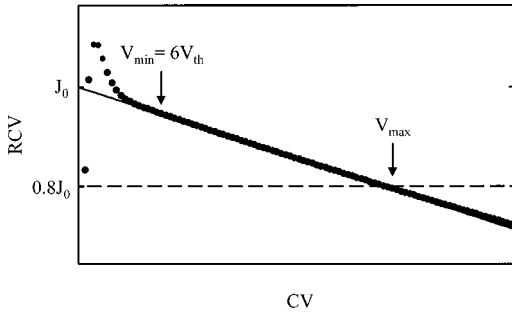
FIG. 2. Theoretical dependence of RCV vs CV. The data are numerically simulated, and the solid line represents the best fit through the data over the prescribed region.

Notice that V_{max} is defined by the product Wd, which means that we can use thinner cells for determination of strong anchoring. We will return to this point below. Hence, within the voltage range

$$V_{min}=6\pi\sqrt{\frac{K_1}{\epsilon_0\epsilon_a}}<V<V_{max}=\frac{0.2Wd}{\cos\theta_p}\sqrt{\frac{\epsilon_\perp}{K_1\epsilon_0\epsilon_a\epsilon_\parallel}},\tag{13}$$

the substitution of Eqs. (4), (5), (9), (10), and (11b) into Eq. (12) predicts a linear dependence of RCV on CV with a coefficient proportional to W^{-1}:

$$RCV=J_0-\frac{J_1}{W}CV.\tag{14}$$

Here

$$J_0=\frac{2\pi n_0\nu\epsilon_0\epsilon_\perp S}{\lambda}\sqrt{\frac{K_1}{\epsilon_0\epsilon_a}}\sqrt{1+\gamma}I_R(y_p,1)$$

and

$$J_1=B_R\frac{2\pi K_1 n_0\nu}{\lambda}\sqrt{\frac{(1+\kappa y_p)(1-y_p)}{1+\gamma y_p}}.$$

Equation (14) allows one to determine W from a simple linear fit. It is valid for any pretilt angle and reduces to the YvS formula[12] with $J_1=[4\pi K_1(n_e-n_0)]/\lambda$ when there is no pretilt, $\theta_p=0$. Numerical calculations show that the simplified formulas with $\theta_p=0$ result in an error less than 0.05 W when $\theta_p<10°$; however, the error grows to $\sim W$ when $\theta_p\sim45°$.

Note that Eq. (13) still requires knowledge of W to determine V_{max}. Since W is not known *a priori*, this can present a difficulty. The upper limit of the fitting range can be estimated from Eq. (14), where one replaces V by V_{max}. To preserve $s_b<0.2$, the second term in Eq. (14) should be less than 20% of the first term, J_0. Thus, V_{max} can be obtained directly from the experimental plot $RCV(CV)$ without resorting to the value of W. First, one estimates J_0 from the intercept of the linear part of the function $RCV(CV)$ for $V>6V_{th}$. Second, V_{max} is defined as the voltage for which RCV becomes 80% of J_0. The process is illustrated in Fig. 2. We will refer to this procedure of finding V_{max} as the 80% rule.

Let us return to the consideration of cell thickness. As stated, the linear fit of RCV as a function of CV must be performed over a prescribed voltage region given by Eq. (13). By defining the electric coherence length, d_E as

$$d_E=\frac{\epsilon_0\epsilon_\parallel S}{CV}\sqrt{\frac{K_1}{\epsilon_0\epsilon_a}},\tag{15}$$

and the anchoring extrapolation length as

$$d_W=\frac{K_1}{W},\tag{16}$$

and noting that in high enough fields ($V>6V_{th}$), the electric coherence length can be estimated as $d_E\approx(V_{th}/\pi V)d$, one can rewrite Eq. (13) as

$$\frac{d}{20}>d_E>3\sqrt{\frac{\epsilon_\parallel}{\epsilon_\perp}}d_W.\tag{17}$$

Hence, to have a fairly large voltage range to fit the data, for a typical nematic such as 5CB, the thickness should be at least 200 times larger than the extrapolation length,

$$d>200d_W.\tag{18}$$

Yokoyama and van Sprang[12] applied these requirements to a substrate with weak anchoring: $W\sim10^{-5}$ J/m² yielding $d_W\sim0.5$ μm.[24] For this W, the cell must be at least 50 μm to yield a significant voltage range to fit the experimental data. However, in many cases,[25] the YvS technique gives W of the order 10^{-4} or 10^{-3} J/m² which makes $d_W\sim10^{-2}$ μm or smaller. If this is the case, it should be possible to use the YvS technique for a thin cell (of the order of μm's) and still satisfy Eq. (17).

B. RV technique

Despite the convenience of a linear fit, a corresponding YvS experiment requires to measure both phase retardation and capacitance. The measurements of capacitance might be especially undesired since they require a cell with patterned electrodes and a uniform thickness over the whole area of the electrodes. Patterning of the electrodes is usually achieved by etching techniques. The etching solutions not only remove the undesired parts of the electrode but also can damage the protected electrode area, by penetrating the protective coating. The damage, along with many other possible factors, contributes to the inhomogeneities of the director orientation which, as we show in Secs. IV and VI, ultimately make the determination of W very inaccurate or impossible. The problem can be avoided if one uses the recently suggested RV technique that does not require etching.

In the RV technique, one measures only the retardation of the cell as a function of applied voltage. However, $RV(V)$ has linear behavior only when C becomes practically constant by reaching a saturation value $C_\infty=(\epsilon_0\epsilon_\parallel S)/d$ at very high field ($V>\tilde{V}_{min}\geq6V_{th}$). This circumstance reduces the range ($\tilde{V}_{min},V_{max}$) significantly. To avoid the problem and to obtain a C-independent function that has the same voltage range of linear behavior as $RCV(CV)$ has, one can use the following relationship

$$CV=\frac{\epsilon_0\epsilon_\parallel S}{Qd}(V-\bar{V}),\tag{19}$$

which follows directly from Eq. (11a). Here

$$Q = 1 - \frac{2K_1}{Wd} \frac{\gamma(1+\kappa y_p)(1-y_p)}{(1+\gamma y_p)},$$

$$\bar{V} = \alpha \frac{\epsilon_a}{\epsilon_\parallel} V_{\text{th}},$$

and

$$\alpha = \frac{1}{\pi} \int_{y_p}^{1} \sqrt{\frac{(1+\gamma)(1+\kappa y)}{y(1+\gamma y)}} \, dy.$$

Equation (19) is valid over the same voltage range $(V_{\min}, V_{\max})$ given in Eq. (13). For most liquid crystals (with positive $\lambda > 0$ and $\kappa > 0$), the coefficient α is between $2/\pi$ and 1. For example, $\alpha = 0.90$ in 5 CB with zero pretilt angle.

Substituting Eq. (19) in Eq. (14) and normalizing by the initial (at zero voltage) phase retardation

$$R_0 = \frac{2\pi d n_0 \nu(1-y_p)}{\lambda(1+\sqrt{1-\nu(1-y_p)})\sqrt{1-\nu(1-y_p)}}, \qquad (20)$$

we obtain the formula which is valid in the voltage range $(V_{\min}, V_{\max})$ specified by Eq. (13) and allows one to determine W from a simple linear fit without capacitance measurements:

$$\frac{R(V-\bar{V})}{R_0} = \tilde{J}_0 - \frac{2K_1}{Wd}(1+\kappa y_p)(V-\bar{V}). \qquad (21)$$

Here

$$\tilde{J}_0 = Q \sqrt{\frac{K_1}{\epsilon_0 \epsilon_a}} \frac{(1+\sqrt{1-\nu(1-y_p)})\sqrt{1-\nu(1-y_p)}}{(1-y_p)\sqrt{1+\gamma}} I_R(y_p, 1).$$

When fitting the experimental data with Eq. (21), $V_{\max}$ can be determined from the requirement that the second term is equal to 20% of the first term, similar to the RCV case above.

Note that Sun and Yokoyama[15] recently suggested to avoid the measurements of C by placing a small capacitor $C_{\text{add}} \ll C$ in series with the nematic cell and then assuming that the total capacitance is a voltage independent constant determined by C_{add}. In contrast, the RV technique obtains the linear behavior of $R(V-\bar{V})$ vs $(V-\bar{V})$ from Eq. (21) that is exact within the range $(V_{\min}, V_{\max})$.

III. MATERIALS AND EXPERIMENTAL TECHNIQUES

A. Preparation of cell

The study of liquid crystal-surface anchoring requires well-prepared cells. We used soda lime glass manufactured by Donnelly Applied Films Corporation with a silicon dioxide barrier and indium tin oxide (ITO) layer. It was acid etched such that to leave the well-defined rectangular patterns of ITO, cleaned in an ultrasonic bath, rinsed with deionized water and electronic grade isoproponal, and then dried in an oven. A 0.75 wt. % solution of the chemically imidized polyimide LARC CP1 (developed by NASA)[26] in dimethylacetamide was spin coated unto the glass. The glass was then baked at 275 °C and mechanically rubbed in one direction with a velvet cloth. Rubbing of this alignment material creates grooves 13–16 nm high.[26] A cell was then formed from two substrates, which were cut from the glass and aligned in such a way that the two rubbing directions were antiparallel and the patterned ITO areas overlapped. Mylar strips were placed between the substrates to form a uniform gap, and the substrates were glued together using 5 min epoxy. The thickness of the cell was measured by interference method (accuracy of 0.1 μm for cells 10–60 μm thick). Still more cells were assembled using the alignment layer HD MicroSystems PI2555. This alignment layer was prepared by spin coating a 1:4 solution of PI2555 in the HD MicroSystems solvent T9039 onto substrates cleaned as above. The substrates were baked for 1 h at 275 °C and mechanically rubbed.

The rubbed polyimide film, strains in the glass and other coatings, might cause an optical phase retardation additional to that of the liquid crystal.[27] For example, this retardation, R_{sub}, was measured by the Senarmont technique to be 0.8° for an empty 47 μm cell which is described later in the text in Secs. IV A and IV B.

The cell was then filled by capillary method with the nematic liquid crystal 4-n-pentyl-4′-cyanobiphenyl (5CB) from EM Industries at a temperature above the nematic-isotropic transition point. The physical properties of 5 CB at 23 °C are: $K_1 = 6.65 \times 10^{-12}$ N and $K_3 = 8.85 \times 10^{-12}$ N;[28] $n_e = 1.717$, $n_0 = 1.530$ measured in the laboratory using an attenuated total internal reflection technique and Abbe refractometry. The dielectric constants of the liquid crystal were measured using the Automated Properties Tester from DisplayTech in cells provided by DisplayTech and by measurement of the capacitance using the Schlumberger SI 1260 Impedance Analyzer. We found $\epsilon_\parallel = 19.1$ and $\epsilon_\perp = 6.3$. Finally, the pretilt angle of the cell was measured by the magnetic null method.[29]

All measurements were made at 23 °C. The heating of the cell due to a high applied voltage was determined to be less than 0.1 °C. This was accomplished by measuring the nematic-isotropic temperature of the liquid crystal, and then lowering the temperature 0.1 °C below that point. A voltage of 60 V was then applied for 16 h, and, in this period, the liquid crystal did not undergo a phase transition to the isotropic phase.

B. Measurement of capacitance

The measurement of capacitance should be performed with special care. Before beginning the YvS experiment, the capacitance and resistance of the liquid crystal cell are determined using a Schlumberger SI 1260 Impedance Analyzer with the applied voltage changing from 0 to 3 V (rms). This serves as an experimental check of the bulk properties of the liquid crystal through determination of the threshold voltage, as well as an accurate measure of the capacitance. Leads are then attached to the cell, and it is placed in the experimental setup for the determination of anchoring. The cell is driven by a Stanford Research Systems Model DS345 function generator amplified by a Krohn–Hite Model 7600 Wide Band Amplifier. The sinusoidal potential is routed into a cell and a
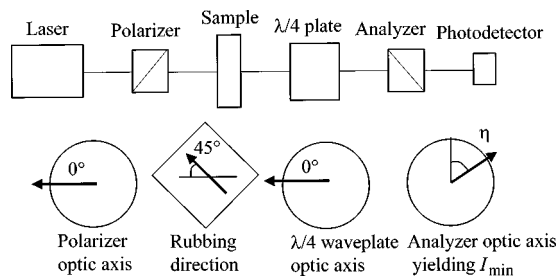
FIG. 3. Experimental setup to measure optical phase retardation by the Senarmont technique. η is the angle of the analyzer for the minimum transmittance I_{min}.

FIG. 4. Relative error $\Delta R/R$ caused by azimuthal misalignment t of the cell as a function of R for $t=1°$ and $t=3°$.

30 kΩ resistor in series, and the potential drop across the resistor is measured. The voltage drop across the resistor is considered when determining the voltage across the cell. Since the resistance of the cells used was larger than 3 MΩ, and, thus, gave negligible contributions to the total impedance, the capacitance of the cell can be determined. Since the leads to the cell also add a capacitance, the results of this experiment are compared with the capacitance measured with the Schlumberger SI 1260 Impedance Analyzer, with the appropriate constant subtracted off of the former results. This method gives the capacitance of the cell to within 1 pF.

C. Measurement of optical phase retardation

The optical phase retardation of the liquid crystal cell is determined by the Senarmont technique (see Fig. 3).[30] The light source was a HeNe laser with an attenuated beam intensity. (Each successive optical element was placed perpendicular to the laser direction.) A second Glan–Thompson polarizer (analyzer) is set up on a motorized rotation stage and rotated into the position of maximum extinction (crossed with the first polarizer). A quarter-wave plate (in our case, a Soleil–Babinet compensator) with its optical axis parallel to the first polarizer is then placed between the two polarizers. The liquid crystal cell is then placed between the quarter wave plate and the first polarizer such that the cell's optical axis (the rubbing direction) is at 45° with respect to the first polarizer.

The linearly polarized light entering the sample emerges elliptically polarized. When the optical axis of the sample is set at 45° with respect to the polarizer, the azimuth of the ellipse is zero with respect to the polarizer. Ideally, setting the optical axis of the quarter-wave plate parallel to the polarizer transforms the elliptically polarized light emerging from the sample into linearly polarized light. The measurement of the azimuth of this linearly polarized light using the analyzer allows for the determination of the phase retardation of the sample. The uncertainty in the azimuthal setting of the sample results in the uncertainty in the measured azimuth of the light transmitted through the quarter-wave plate, and hence the uncertainty in the measurement of the optical phase retardation.

Let us suppose that the optical axis of the sample is at a small angle t from the 45° position. Then the light transmitted through the quarter-wave plate remains slightly ellipti-
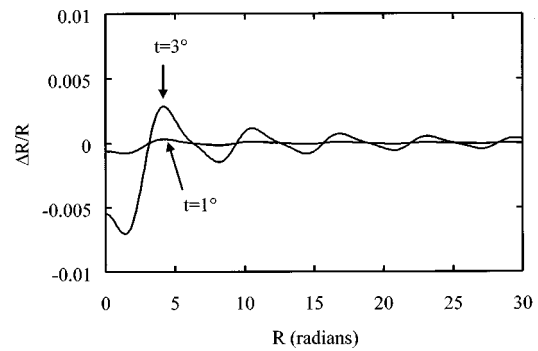
cally polarized. The ellipticity and azimuth of the light can be found using the Mueller matrix formalism. For the azimuth η, we have

$$\eta = \frac{1}{2}\tan^{-1}\left[\frac{\cos(2t)\sin\delta}{\sin^2(2t)+\cos^2(2t)\cos\delta}\right], \qquad (22)$$

where δ is related to the total phase retardation R by $R = 2\pi N + \delta$ (N is an integer). When the uncertainty in the azimuthal setting t goes to zero, then the relation $\delta = 2\eta$ holds. The relative uncertainty in the phase retardation measurement ΔR is a function of δ and t, and can be calculated to be

$$\frac{\Delta R}{R} = \frac{1}{R}\left\{\tan^{-1}\left[\frac{\cos(2t)\sin R}{\sin^2(2t)+\cos^2(2t)\cos R}\right]-\delta\right\}. \qquad (23)$$

In Fig. 4, we have plotted $\Delta R/R$ as a function of R for $t = 1°$ and $t = 3°$. The accuracy of the azimuthal setting of the cell in our experiment is better than 1°, hence, the corresponding relative uncertainty in the measured optical phase retardation is less than 0.1%. To check the accuracy experimentally, we rotated the crossed polarizers and the quarter-wave plate 3° with respect to the sample and measured the retardation of a nematic cell as a function of applied voltage. Comparing the results with those previously obtained with the correct settings, no distinguishable difference in the dependence $R(V)$ was found.

During the measurement, the analyzer is rotated to determine the azimuth of the linearly polarized light emerging from the quarter wave plate by finding the angle of maximum extinction. After the potential has been applied to the cell, this angle is located in three steps. First, the analyzer is rotated between 0° and 180° with the intensity measured every 10°. The analyzer angle corresponding to the minimal intensity is identified, and the analyzer is then rotated by steps of 1° from 10° less than the angle of minimal intensity to 10° more than the angle of minimal intensity with the intensity being measured at each point. With the angle of minimal transmission identified, the last step is repeated for steps of 0.1° from 1° less than the angle of minimal intensity to 1° more. This analyzer angle σ_{min} yielding minimum transmission equals η, and the optical phase retardation is given by two times σ_{min} plus an integer factor of 2π. This entire process takes three minutes. To assure the liquid crys-

tal in the cell was in its equilibrium distribution, a 30 min delay between experimental points was attempted with no change in the experimental results.

Besides the possible uncertainty due to azimuthal setting of the cell, there are other possible sources of error in measurement of retardation. First, since the impinging light is polarized at 45° with respect to the liquid crystal director at the surface, the reflection coefficient will be different for the light polarization parallel to the director and perpendicular to the director. This effect can be important if the reflection coefficients are large. To measure the reflection coefficient, the analyzer was removed and the light intensity was measured as a function of applied voltage. The change in light intensity for applied voltages up to 80 V was 2%. Numerical estimates show that a 2% change in the intensities of ordinary and extraordinary waves give a 1% change in ellipticity of the transmitted light, leading to a 0.5° error in phase retardation. Therefore, the effect of the phase retardation changes due to multiple-beam interference can be neglected.

Finally, there is the possibility of the cell changing thickness as a result of attractive or repulsive electric interactions between the substrates. To check this, an empty cell's thickness was measured as a function of applied voltage and found not to change.

Summarizing this section, we have established that there is an absolute uncertainty in the measured optical phase retardation of 0.5°.

IV. EXPERIMENTAL RESULTS USING HIGH-ELECTRIC-FIELD TECHNIQUE

A. Yokoyama–van Sprang technique

In this section, we present experimental results for a liquid crystal cell in which the straightforward application of the standard YvS technique does not allow for unambiguous measurement of W.

Our first example is a cell with carefully prepared and uniformly buffed NASA LARC CP1 alignment layers. The cell thickness was 47.2 μm and pretilt was 0.4°. Recall from Sec. II, the retardation caused by director configuration is obtained from Eq. (14) as

$$R = \frac{J_0}{CV} - \frac{2\pi B_R K_1 n_0 \nu}{\lambda W}. \tag{24}$$

The experimentally measured retardation R_{exp} is the sum of R and R_{sub}, as discussed in Sec. III A:

$$R_{\text{exp}} = \frac{J_0}{CV} - \frac{2\pi B_R K_1 n_0 \nu}{\lambda W} + R_{\text{sub}}. \tag{25}$$

With the constant $R_{\text{sub}} = 0.8°$ (see Sec. III A), the optical phase retardation appears to be a linear function of $1/CV$ (see Fig. 5) (the frequency of the potential was 10 kHz). Following the standard YvS procedure,[12] namely, performing a linear fit of the dependence R vs $1/CV$, W can be determined using Eq. (25). However, the obtained W turns out to be highly dependent on the voltage range chosen over which to make a fit (see Table I), while, in each case, satisfying Eq. (13) and, technically speaking, the 80% rule suggested in Sec. II A.
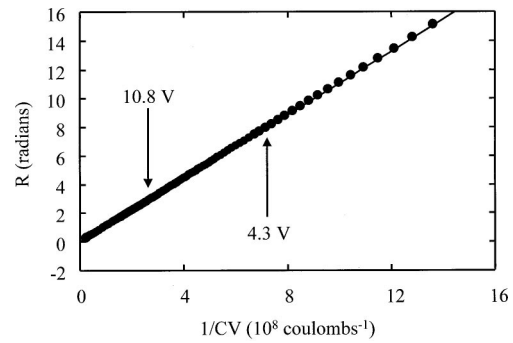

FIG. 5. Retardation R vs $1/CV$ for the 47 μm cell with the NASA LARC CP1 alignment layers. The solid line represents the best fit from 4.3 to 10.8 V.

Graphic appearance of the function R vs $1/CV$, such as in Fig. 5, masks the problem of the voltage-dependent W since this function is close to a straight line for a broad range of W values, and the intercept of this line with the R axis that defines K_1/W is very close to the origin. As a result, small deviations from the ideal linear behavior, hardly seen in the experimental plots R vs $1/CV$ in Fig. 5, would greatly affect the extrapolated location of the intercept and thus the measured W.

To understand the sensitivity of the measured value of W to the limiting voltage for the linear fit, it is useful to rewrite Eq. (25) as

$$(R_{\text{exp}} - R_{\text{sub}})CV = J_0 - \frac{2B_R K_1 n_0 \nu}{\lambda W}CV \tag{26}$$

and to plot the experimental data as $(R_{\text{exp}} - R_{\text{sub}})CV$ vs CV (see Fig. 6, where $R_{\text{sub}} = 0.8°$) and use Eq. (26) to determine W. Since W is expected to be positive, the slope of $(R_{\text{exp}} - R_{\text{sub}})CV$ vs CV should be negative. In the experimental plot, there are few regions with negative slopes, which could yield a positive W. The first is that below 4.0 V, i.e., very near the threshold voltage ($V_{\text{th}} = 0.73$ V), in violation of voltage fitting regime suggested by Yokoyama.[12] The second is from 4.3 to 10.8 V. Above 10.8 V, the slope becomes positive. Thus, any fits over the region from 10.8 to 120 V, which is formally allowed by Eq. (13), would yield infinite or negative W according to Eq. (14). This is similar to the experimental results obtained by Ji and co-workers (see Fig. 4 of Ref. 21), where positive slopes of the experimental plots of RCV against CV were observed at high voltages. As a further illustration, the dependences of RCV vs CV calcu-

TABLE I. Fitted value of W for the 47.2 μm cell over different ranges of ($V_{\text{min}}, V_{\text{max}}$), where we have taken $R_{\text{sub}} = 0.8°$. Note that in each case, Eq. (13) is satisfied.

Voltage range ($V_{\text{min}}, V_{\text{max}}$)	Fitted value of W ($\times 10^{-4}$ J/m^2)	Does this W and voltage range satisfy Eq. (13)?
(4.3 V, 10.8 V)	4.5	Yes
(4.3 V, 25 V)	6.8	Yes
(8 V, 25 V)	13.4	Yes
(8 V, 50 V)	20.1	Yes
(8 V, 100 V)	−146.0	Yes

FIG. 7. Voltage dependence of retardation for the 47 μm cell with the NASA LARC CP1 alignment layers. The solid line represents the numerical calculation for infinite anchoring.
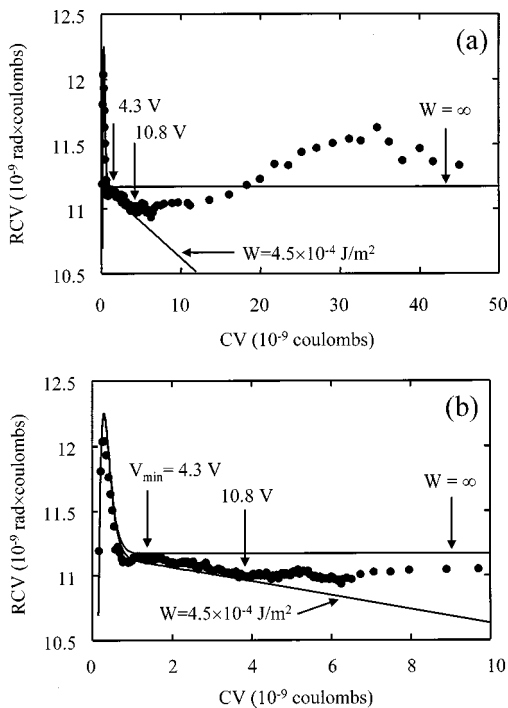
FIG. 6. RCV vs CV for the 47 μm cell with the NASA LARC CP1 alignment layers over (a) the entire voltage range (up to 120 V), and (b) only up to 15 V. The solid lines represent the numerical calculations of the data with $W = \infty$ and $W = 4.5 \times 10^{-4}$ J/m^2.

lated numerically from Eq. (12) with $W \rightarrow \infty$ and $W = 4.5 \times 10^{-4}$ J/m^2 are represented by the solid lines shown in Fig. 6. Between 4.3 and 10.8 V, the data follow the line $W = 4.5 \times 10^{-4}$ J/m^2 quite closely. However, at $V > 10.8$ V, the data cease to provide any meaningful information about W within the frame of the linear-fit model.[12]

As we demonstrated above, one can obtain a wide range of values for W by choosing different V_{max} and still preserving the validity of Eq. (13). The implication of this result is fundamental: the real cell does not behave in the manner expected from the model described in Ref. 12 and in Sec. II.

To trace the source of the discrepancy between the experiment and the theory, the individual data sets, R and C as a function of V, can be fit numerically by the ''exact'' theoretical model, Eqs. (4)–(9), with no assumption about the voltage range. Figure 7 shows the dependence $R(V)$ with the solid line indicating the numerical calculation for infinite anchoring. The measured retardation is larger than the theoretical R for infinite anchoring. The behavior of C with V is much harder to analyze. The measurements imply averaging of the director distribution over a large area of the electrodes,
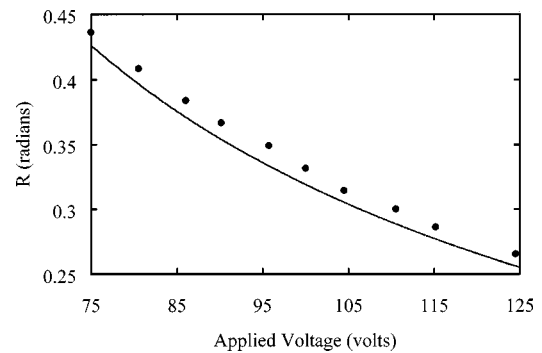
and require very exact knowledge of the dielectric permittivity of the liquid crystal (see Ref. 8 for details). Anyway, the analysis of separate sets of data tells us that at least $R(V)$ does not behave in experiments as it is expected from the theory: the experimental retardation is larger than in the theory (even if the parasitic sources such as R_{sub} are taken into account).

This discrepancy R_x between the experimental and theoretical values of R is not small. It takes at least $R_x = 3°$ to be subtracted from R_{exp} to alter the slope $RCV(CV)$ from positive to negative. Moreover, even this subtraction still leaves W highly dependent on (V_{min}, V_{max}); see Table II and Fig. 8. To force W to be voltage independent, one has to assume that R_x increases at high voltages. The validity of such an arbitrary adjustment of the experimental data is highly questionable, since, first, R_{sub} is significantly smaller than 3°, and, second, R_{sub} should not increase with V. In other words, the discrepancy is caused by some physical process in the nematic cell that is not accounted for in the theoretical model.

The intrinsic problem of the determination of W from the behavior of $RCV(CV)$ or $R(V)$ arise not only in thick cells or in cells with LARC CP1 coatings. We have tested many cells and found the phenomenon of excess retardation to be quite common.

B. Determination of *W* by RV technique

In the previous work,[16] we have demonstrated that the RV and YvS technique give the same values of W when the cell behaves as expected by the theory. We will begin this section by showing that, when the cell behavior deviates

TABLE II. Fitted value of W using Eq. (14) with different amounts of R_x subtracted off, and over different voltage ranges.

	(4.3 V, 10.8 V)	(4.3 V, 25 V)	(8 V, 25 V)	(8 V, 50 V)	(8 V, 100 V)
$R_x = 0°$	$W = 4.5 \times 10^{-4}$ J/m^2	6.8	13.4	20.1	-146.0
$R_x = 1°$	3.4	4.5	6.9	8.3	15.7
$R_x = 2°$	2.8	3.5	4.6	5.2	7.4
$R_x = 3°$	2.3	2.8	3.5	3.8	4.9
$R_x = 5°$	1.7	2.0	2.3	2.5	2.9

from the theory, the RV technique fails to produce the meaningful determination of W, and, in this case, it is no better than the YvS technique.

1. 47 μm NASA LARC CP1 cell

We use the experimental results for the 47 μm cell with NASA LARC CP1 alignment layers described in the previous Sec. IV A. Figure 9 shows $R(V-\bar{V})$ plotted against $(V-\bar{V})$ for this cell. As can be seen, there is again relatively narrow region $(4.3\,\text{V}<V<10.8\,\text{V})$ where the slope is negative. Using Eq. (21) to fit over this region, we obtain W to be 4.3×10^{-4} J/m^2 with $\bar{V}=0.46$ V. This compares well with the result obtained for the same voltage region using the YvS technique $(W=4.5\times10^{-4}$ J/m$^2)$. At applied voltages larger than 10.8 V, the slope is positive, and hence would yield a negative value of W. These results mirror those given in Fig. 6 and Sec. IV A, where the YvS technique was used.

2. 21 μm PI2555 cell

We continued with cells aligned by the standard polyimide layer DuPont PI2555. The first cell was prepared as described in Sec. III including patterned electrodes, and its thickness was 21 μm. The pretilt angle of the cell was measured to be 3.0° by the magnetic null method. To ensure that there was no hybridity within the cell, the pretilt angle was measured with the laser incident upon the cell in three different directions.[31] This allowed us to raise the accuracy of the pretilt measurements to ~0.1°. We noticed, however, that the pretilt angle changes by up to 1° when one probes different locations within the cell.

Greater care was taken to ensure temperature control and azimuthal setting. In this experiment, the temperature of the cell was fixed by a hot stage at (23.000 ± 0.002) °C. The azimuthal setting was achieved by placing the cell between the cross polarizers and compensator and rotating the crossed polarizers and compensator until the light passing through the setup was extinct. Then the polarizers and compensator were rotated 45° to be in proper azimuthal alignment to measure the retardation by the Senarmont technique. R_{sub} was determined as the optical phase retardation of the filled cell at 39 °C, well above the nematic-isotropic transition, and found to be 0.6°.

FIG. 9. $R(V-\bar{V})$ vs $(V-\bar{V})$ for the 47 μm cell with the NASA LARC CP1 alignment layers. The solid line represents the best linear fit over the voltage region from 4.3 to 10.8 V, and yields $W=4.3\times10^{-4}$ J/m^2.

The optical phase retardation of this cell was measured with applied voltages (with a frequency of 10 kHz) between 0.5 and 30 V. Figure 10 shows $R(V-\bar{V})$ plotted against $(V-\bar{V})$. As we can see, there is no region above $6V_{\text{th}}$ in which the slope of the line is negative. Hence, any fit will yield a negative W. This behavior apparently correlates with in-plane director inhomogeneities present in the cell that are visible in polarizing microscopy. Figure 11 shows the textures of the cell with different applied voltages when the optical axis of the cell is parallel and nearly parallel to the polarizer. Even at a large voltage of 10 V, the inhomogeneities are clearly visible.

3. 15 μm PI2555 cell

There are many possible causes of the in-plane inhomogeneities of the cells. Etching of the electrodes is one of them, as the comparison of atomic force microscopy textures in Fig. 12 clearly demonstrates. In addition, electric resistance across the etched electrodes was measured to be larger than that of nonetched electrodes, which further indicates the damage inflicted on the ITO layer by etching.

An important feature of the RV technique is that it does not require patterned electrodes since no measurement of C are needed. In what follows, we describe a cell with nonetched electrodes and show that the discrepancies between the theoretical and experimental functions $R(V)$ is greatly reduced.
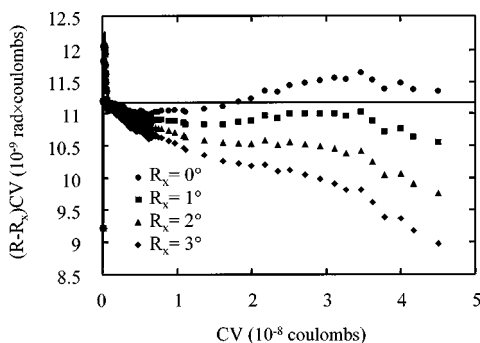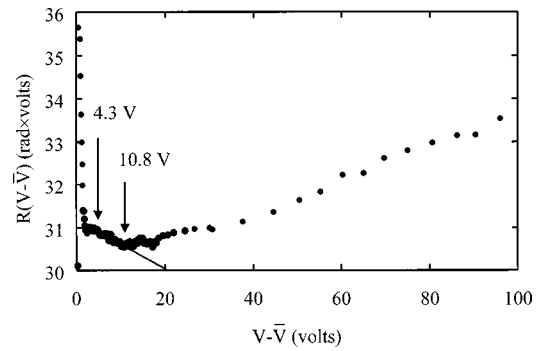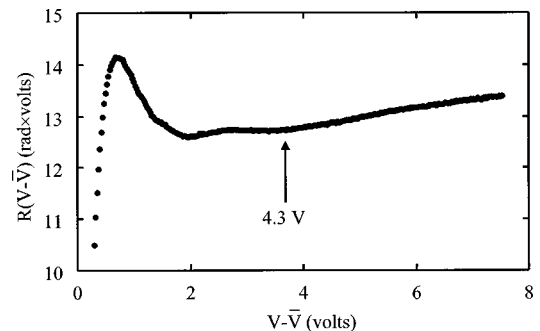

FIG. 8. RCV vs CV with different amounts of excess retardation, R_x, subtracted off for the 47 μm cell with the NASA LARC CP1 alignment layers. The solid line represents the numerical calculation for infinite anchoring.

FIG. 10. $R(V-\bar{V})$ vs $(V-\bar{V})$ for the 21 μm cell with the PI2555 alignment layers. Note that when $V>4.3$ V that the slope is always positive.
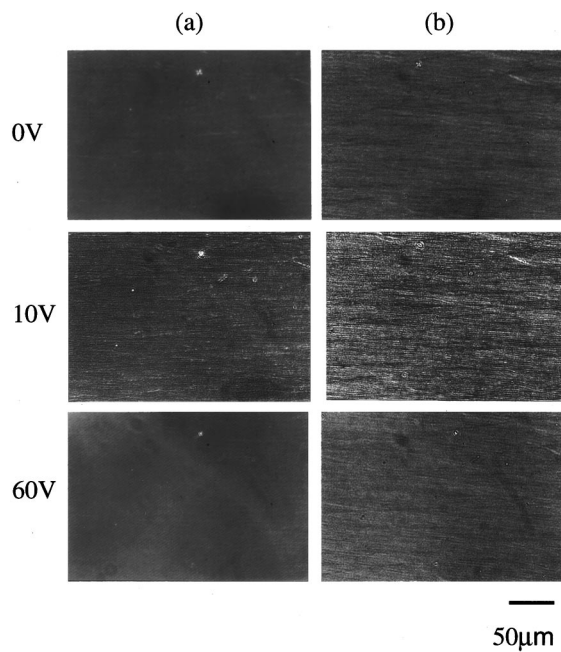
(a)   (b)

0V

10V

60V

50μm

FIG. 11. Polarizing microscopy textures of the 21 μm cell with PI2555 alignment layers at applied voltages of 0, 10, and 60 V: (a) the rubbing direction parallel to the polarizer or (b) the rubbing direction rotated 2° from the polarizing direction of the polarizer.

A cell was created with PI2555 alignment layers and a thickness of 15 μm. Figure 13 shows $R(V-\bar{V})$ vs $(V-\bar{V})$ for this cell with a field frequency of 100 kHz. The slope is negative at $V>6V_{th}$. Using Eq. (21) to fit the experimental data from 4.3 to 8 V (with the 80% rule applied), W is determined to be 7×10^{-5} J/m^2. (Similar results were obtained for potential frequencies at 10 kHz.) When $V=13$ V, the director totally reorients and the measured phase retardation becomes zero as expected from the model. Note here that we never observed such reorientation and steep drop of R in any of the cells with etched electrodes, even at voltages as high as 300 V.

4. 15 μm NASA LARC CP1 cell

Another study was performed on a 15 μm NASA LARC CP1 cell without etched electrodes. The cell was driven with a 100 kHz potential, and the retardation was measured as a function of voltage. The experimental data were fitted using Eq. (21) over the appropriate voltage window (4.3 V$<V$ <7.5 V), and yielded $W=5\times10^{-5}$ J/m^2. Also, the measured
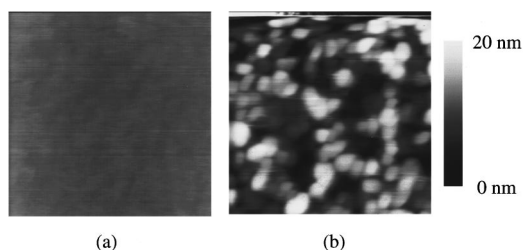

20 nm

0 nm

(a)   (b)

FIG. 12. Contact-mode atomic force microscopy images of (a) nonetched and (b) etched substrates. The image is 1 μm square, and the full gray scale represents height variations of 20 nm.
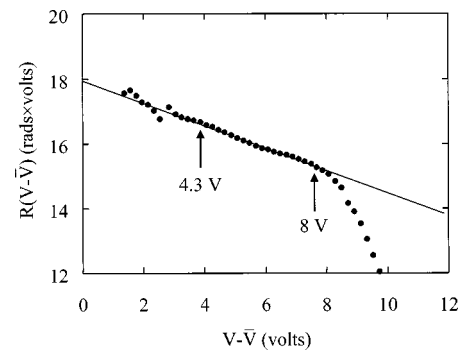

FIG. 13. $R(V-\bar{V})$ vs $(V-\bar{V})$ for the 15 μm cell with the PI2555 alignment layers. The solid line represents the best fit of the $R(V-\bar{V})$ vs $(V-\bar{V})$ from 4.3 to 8 V, yielding $W=7\times10^{-5}$ J/m^2.

phase retardation becomes zero at 13 V manifesting total director reorientation as expected from the model.

It appears from all the experiments above that the problem of ''unmeasurable'' W (the 47 and 21 μm cells) is related to in-plane inhomogeneities. We will revisit this question in Sec. VI with a quantitative analysis. In contract, the two 15 μm cells with non-etched electrodes behave in a way predicted by the theory and show well-defined values of W. It is thus of interest to employ an independent technique for comparison.

V. THE ESTIMATION OF *W* FROM THE FREDERIKS THRESHOLD

The threshold voltage V_{th}^W of the Frederiks transition in liquid crystal cells depends on the anchoring strength.[5] This feature has been utilized by Rosenblatt and co-workers[7,9] to determine W by comparing the thresholds in thick and thin cells[7] or by measuring the threshold in a wedge cell.[9] The relationship between W and V_{th}^W in approximation of the Rapini–Papoular anchoring potential for a planar cell with no pretilt reads[32]

$$V_{th}^W \sqrt{K_1 \epsilon_0 \epsilon_a} \tan\left(\frac{V_{th}^W}{2}\frac{\epsilon_0 \epsilon_a}{K_1}\right) = dW. \tag{27}$$

The l.h.s. of Eq. (27) can then be plotted as a function of thickness, d. The value of K_1 can be adjusted to cause the data to fall into a straight line with zero intercept, and the slope of this line will yield W.[9]

Even in the case of no measurable pretilt, the threshold location can be difficult to determine since any measured property of the liquid crystal cell changes gradually, not drastically, near the threshold voltage. Experimentalists working in this field determine the threshold by a double extrapolation (i.e., a linear extrapolation of the data before the onset of the threshold and after the onset of the threshold) of the experimental data, with the intercept yielding V_{th}^W. Our situation is further complicated because of small (0.3°) pretilt. By the same extrapolation method, we can determine an apparent threshold value.[33] For any given thickness and using the known value of K_1, this apparent threshold will always underestimate the value of W, however, we wish to
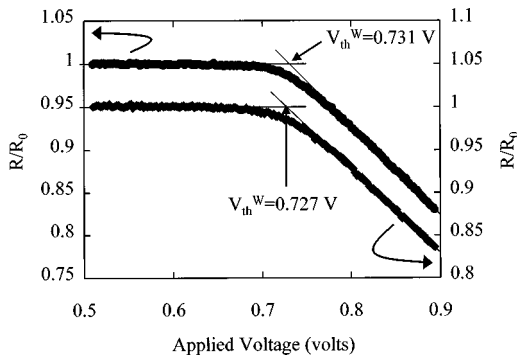
FIG. 14. Normalized phase retardation as a function of applied voltage. The top set of the data is at $d=8.2\ \mu$m and the bottom set is at $d=3.7\ \mu$m (shifted down). The lines represent the double extrapolation method, with the intercept representing the apparent threshold voltage.

FIG. 15. Apparent threshold voltage vs local thickness for the wedge cell with the NASA LARC CP1 alignment layers.

apply the wedge-cell technique[9] where the apparent threshold will be measured at many thickness and this data will be analyzed as a group, not individually.

We performed a computer ''experiment'' to examine if measuring the apparent threshold at several thicknesses of a wedge cell with nonzero pretilt can yield an accurate value of W. Numerical data, representing theoretical dependence of the optical phase retardation, R vs applied voltage V in the vicinity of $V_{\mathrm{th}}=\pi\sqrt{K_1/(\epsilon_0\epsilon_a)}$ were simulated using Eqs. (4) and (5). The double extrapolation method was applied to the $R(V)$ to determine the apparent threshold at several thicknesses. This apparent threshold was used in the l.h.s. of Eq. (27), and the l.h.s. of Eq. (27) was plotted against the local thickness d. K_1 was then adjusted to give the best straight line, with the slope giving the value of W. The numerically simulated data with $\theta_p=0.5°$ gave the correct value of W (with an error of 10% when $W=1\times10^{-4}$ J/m^2), and a reduced (by 5%) value of K_1. Thus, the accuracy is satisfactory to employ the technique in real experiments.

To run the real experiment, we prepared a wedge cell with LARC CP1 alignment layers on etched ITO substrates. The wedge was created by placing a 12 μm Mylar strip on one side between the substrates such that the rubbing direction was parallel to the direction of uniform thickness. The substrates were pressed together and glued using 5 min epoxy. The interference fringes of the empty cell parallel to the wedge apex reveal the uniform change in thickness from the apex to the spacer. The cell was filled with 5CB along the direction of uniform thickness above the nematic-isotropic transition temperature.

The optical phase retardation of the cell was measured as a function of applied voltage at several points along the wedge. The diameter of the laser beam was approximately 1 mm. The value of R_0, the retardation measured at zero voltage was determined by averaging all the data points taken below 0.6 V. The local thickness can be calculated from the value of R_0 using Eq. (20) with knowledge of the optical anisotropy. Figure 14 shows the threshold voltage as determined by linearly fitting the experimental optical phase retardation as a function of applied voltage from 0.8 to 0.9 V and finding the intercept with $R=R_0$. Figure 15 plots the apparent threshold voltage as a function of wedge thickness.
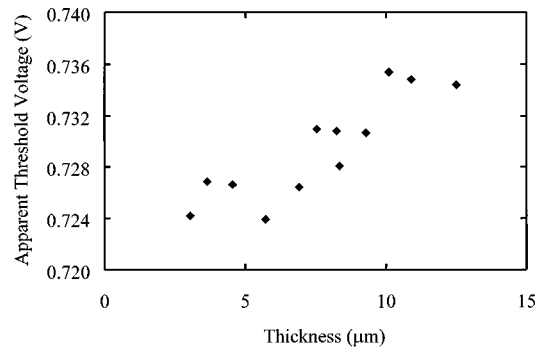
The experimental data were plotted with l.h.s. of Eq. (27) against thickness (see Fig. 16). The best fit of K_1 and W was performed, yielding $K_1=6.4$ pN and $W=(1\pm0.5)\times10^{-4}$ J/m^2. The last quantity compares fairly well with W obtained by the RV technique for the 15 μm cell (NASA LARC CP1 coating) but is absolutely out of the range of W values obtained for the 47 μm cell (where $W=4.3\times10^{-4}$ J/m^2, higher, or even negative, depending on the voltage range). Table III summarizes all the experimental findings on W for comparison.

VI. DISCUSSION

Facing the problem of negative values of W obtained using the YvS technique, Yokoyama suggested[20] that the additional surface orientational order should be taken into account as a possible source of excess retardation. Our experimental cells, heated to temperature above the nematic-isotropic point T_{NI}, show that the phase retardation caused by non-vanishing surface nematic order is less than 1°. Similar results by Kim and Rosenblatt[27] indicate that rubbing-induced phase retardation might achieve 3° just above T_{NI}. Numerical calculations (based on the Maier–Saupe model) of the surface-induced order[34] show that the corresponding phase retardation is significantly smaller (at least four times) in the nematic phase than in the isotropic phase. Therefore, it is highly unlikely that the surface-enhanced order alone can explain the rather large discrepancy between experimental
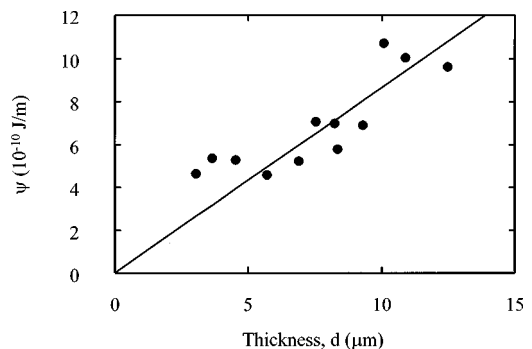

FIG. 16. Dependence of $\psi=V_{\mathrm{th}}^W\sqrt{K_1\epsilon_0\epsilon_a}\tan[(V_{\mathrm{th}}^W/2(\epsilon_0\epsilon_a/K_1)]$ on the local thickness d for the wedge cell with the NASA LARC CP1 alignment layers. The line represents the best fit of the data giving $W\approx10^{-4}$ J/m^2 and $K_1=6.4$ pN.

TABLE III. Polar anchoring coefficient W for different cells described in this article.

Cell thickness	Alignment layer	Electrodes	W (10^{-4} J/m^2) (technique)
47 μm	NASA LARC CP1	etched	between 4.3 and ∞ or negative, depending on the voltage range (YvS and RV)
21 μm	PI2555	etched	negative (RV)
15 μm	P12555	not etched	0.7 (RV)
15 μm	NASA LARC CP1	not etched	0.5 (RV)
Wedge	NASA LARC CP1	etched	1 ± 0.5 (Fredericks threshold)

and theoretical retardation observed in some cells. Especially difficult is to explain why this discrepancy increased with voltage, as observed in the 47 μm cell with NASA LARC CP1 alignment layers. Note that Stallinga *et al.*[22] also observed the discrepancy in experimental and theoretical retardation. Their careful analysis demonstrated that such factors as multiple reflections and flexoelectricity cannot explain the effect.

Section IV B indicates that the unphysical values of W (such as negative or voltage-dependent W's) might be caused by in-plane inhomogeneities. Below in Sec. VI A, we present direct experimental evidence that the spurious results of YvS and RV techniques can result from in-plane surface inhomogeneities that are not taken in account by the theoretical model. In Sec. VI B, we describe a protocol designed to test if a particular cell can be used to measure W by the YvS or RV technique.

A. In-plane inhomogeneities

One of the strongest assumptions of the YvS technique and of the theoretical analysis in this article is that the director configuration is one-dimensional $\mathbf{n} = \mathbf{n}(z)$, $n_y = 0$, and n_x, n_z do not depend on the in-plane coordinates (x,y). In real cells, however, the director is generally nonuniform: $n_{x,z} = n_{x,z}(x,y,z)$ and $n_y \neq 0$. We first demonstrate that the director is nonuniform even when there is no external field. This director inhomogeneity can be tested by the Senarmont technique.

The transmittance T of the cell with both azimuthal and polar variations in $\mathbf{n}$ can be derived using Mueller matrix formalism to be

$$T = \frac{I}{I_{\max}}$$

$$= \frac{1}{2} \langle 1 - \cos(2\sigma - \delta)\cos 2\xi$$

$$- \cos 2\sigma [\cos 2\xi \cos \delta (1 - \cos 2\xi) - \sin^2 2\xi] \rangle. \quad (28)$$

Here $\langle ... \rangle$ means the average over the beam cross section. Also, I is the intensity of the light passing through the polarizer, cell, quarter-wave plate, and analyzer, $I_{\max}$ is the intensity of the light after the polarizer, σ is the angular deviation of the analyzer from its 90° position with the polarizer, δ

$= \delta(x,y)$ is related to the local phase retardation through $R = 2\pi N + \delta$ and $\xi = \xi(x,y)$ is the local azimuthal deviation of the director from the averaged easy axis (aligned at 45° with respect to the polarizer).

If the nematic cell were perfectly uniform, $\xi = 0$ and $\delta = $ constant (i.e., ξ and δ do not depend on x,y), then the minimum transmitted intensity $T_{\min}$ achieved at the proper analyzer orientation ($\sigma_{\min} = \delta/2$) is zero. However, our experiments clearly show that $T_{\min}$ is never zero, even when all of the parasitic effects (such as dark current of the photodetector) are taken into account or even overestimated. The excess transmittance T_{ex}, defined as the difference between $T_{\min}$ and the transmission through the apparatus with crossed polarizers and the sample removed, is caused by director inhomogeneity. As easy to deduce from Eq. (28), any director deviation [i.e., when ξ or δ depend on (x,y)] cause an increase in T_{ex}.

Our measurements indicate that in very well-aligned samples, $T_{\mathrm{ex}} \sim 10^{-4}$ or less. The most intriguing feature is that T_{ex} in some well-prepared samples can dramatically increase when the voltage is applied. Moreover, the increase in T_{ex} with V correlates with the appearance of positive slopes of dependencies such as RCV vs CV, which are responsible for the unphysical (negative) values of W. Figure 17 helps to illustrate the statements above. It shows how T_{ex} increases with V for two cells with the thicknesses $d = 21$ μm and $d = 15$ μm, used in Sec. IV B. In both cases, one deals with a
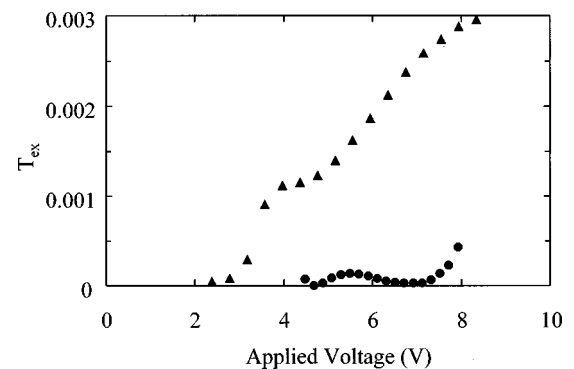

FIG. 17. Voltage dependence of T_{ex} for two cells with PI2555 alignment layers: cell of thickness $d = 21$ μm, etched electrodes (triangles); cell of thickness $d = 15$ μm, nonetched electrodes (circles).

J. Appl. Phys., Vol. 86, No. 8, 15 October 1999

Nastishin *et al.*   4211

PI2555/5CB interface. In the 21 μm (etched) cell, T_{ex} increases with V approximately to 4×10^{-3} at $V=20$ V. This very same cell shows a positive slope of $R(V-\bar{V})$ vs $(V-\bar{V})$ (see Fig. 10). In contrast, the 15 μm (nonetched) cell shows a much smaller T_{ex} in the region (4.3 V$<V<8$ V) needed for the fitting procedure. Note that the $R(V-\bar{V})$ vs $(V-\bar{V})$ plot for this cell has a negative slope (see Fig. 13) implying a positive-definite W.

As already discussed in Sec. IV A, the positive slope of $R(V-\bar{V})$ vs $(V-\bar{V})$ plots and related plots such as RCV vs CV can be explained by some excess retardation R_x. For example, the RCV vs CV plot for the 47 μm cell in Sec. IV A can be fit by the YvS model only if R_x is larger than $3°$ and increases with V. Therefore, both T_{ex} and R_x can result from the same physical reasons, namely, from the in-plane director inhomogeneity. On the other hand, in the 15 μm cell, the slope of $R(V-\bar{V})$ vs $(V-\bar{V})$ is negative alleviating the need to introduce R_x to resolve the experimental and theoretical data. As expected, T_{ex} is relatively small in this cell ($\leqslant 5\times 10^{-4}$) in the voltage region (4.3 V$<V<8$ V) where the fit was performed.

The value of T_{ex} strongly affects validity of the results produced by YvS or RV techniques. Nonzero T_{ex} leads to overestimation of W obtained by fitting the phase retardation data with Eq. (14) or Eq. (21). In other words, the effect is similar to that of excess phase retardation R_x described in detail in Sec. IV A for 47 μm cell. Here, R_x can be understood as the difference between the retardation measured by finding σ_{min} in the experiment and the real retardation average over the beam's cross section. Unlike R_x, the value of T_{ex} can readily be determined experimentally. One might thus wonder if there is a possibility to adjust the experimental data by finding R_x from the measured T_{ex}. Unfortunately, the exact relationship between R_x and T_{ex} depends on the details of director inhomogeneities and cannot be found as a universal function. Nevertheless, one can roughly estimate what kind of errors is expected for different T_{ex}.

For small deviations, the values of R_x and T_{ex} can be expanded in series as

$$T_{ex}=a_1\langle\xi^2\rangle+a_2\langle(2\sigma_{min}-\delta)^2\rangle, \tag{29}$$

$$R_x=b_1\langle\xi^2\rangle+b_2\langle(2\sigma_{min}-\delta)^2\rangle; \tag{30}$$

the linear terms drop out because in the experiment, one sets $\sigma_{min}=\langle\delta/2\rangle$ to get the minimum of T. The contribution of the cross term of $\sqrt{\langle\xi^2\rangle}$ and $\sqrt{\langle(\delta-2\sigma_{min})^2\rangle}$ to Eq. (30) when azimuthal and polar inhomogeneities coexist can be neglected. For example, at $\sqrt{\langle\xi^2\rangle}=3°$ and $\sqrt{\langle(\delta-2\sigma_{mn})^2\rangle}=10°$, then from Eq. (28), the effect of a cross term in Eq. (30) would be less than $0.6°$. According to Eq. (28), a_1 and a_2 are positive definite. Furthermore, b_1 should be negative when $R<\pi$. Therefore, it is not likely that azimuthal inhomogeneities are responsible for the unusual (positive) slopes of RCV vs CV or $R(V-\bar{V})$ vs $(V-\bar{V})$: in the experiment, these positive slopes are accompanied by the increase of T_{ex} with V. On the other hand, polar inhomogeneities such as variations in the local values of $W=W(x,y)$, $\theta_p=\theta_p(x,y)$, electric surface polarization, etc., as well as fractures in the electrode surface, might increase both T_{ex} and R_x simultaneously. Really, the polar variations create in-plane gradients of the dielectric permittivity and, therefore, nonzero in-plane component of the electric field $E_x\neq 0$. This in-plane field tends to deviate the director towards the substrate. Since n_e-n_0 is positive, the corresponding correction to R should be positive. The in-plane field may also prevent total reorientation of the director at high voltages. Another possibility is that in a high electric field, the subsurface nematic layers adopt hybrid-aligned geometry which might enhance in-plane director distortions as discussed in Ref. 35.

Let us return to the problem of quantitative estimates of T_{ex},R_x and related errors in W. First, as follows from Eq. (29) and Eq. (30), $R_x\approx kT_{ex}$, where k is an unknown coefficient. Strictly speaking, k is voltage dependent, but, for our estimates, we assume it to be constant. To yield a positive definite W, $R_x\approx 10°$ for the 21 μm cell. As measured for the same cell, $T_{ex}\sim 10^{-3}$. Hence, small $R_x\approx 1°$ would correspond to $T_{ex}\sim 10^{-4}$. Second, with known R_x, the error in W can be estimated from Eq. (14) or Eq. (21). This error depends both on R_x and W. When $R_x\sim 1°$, the overestimate of W is 1% for $W=10^{-5}$ J/m^2, 10% for $W=10^{-4}$ J/m^2 and much more than 100% for $W\geqslant 10^{-3}$ J/m^2. Thus, to characterize a strongly anchored cell with $W\sim 10^{-4}$ J/m^2, one has to have $T_{ex}\sim 10^{-4}$ or smaller.

B. Protocol to verify the validity of the YvS and RV techniques

We propose a protocol to characterize the nematic cell and to ascertain if the cell can be used for the determination of W by YvS or RV technique. In general, the RV technique is favorable since not only does it eliminates several experiment steps that the YvS technique requires, but it also does not require patterned electrodes which could add in-plane inhomogeneities.

A liquid crystal cell should be assembled with the alignment layers antiparallel to one another. The following steps need to be undertaken to use the YvS or RV technique.

1. Verification and nulling of the phase retardation setup

Determine the minimum signal of the photodetector I_{dark} with the polarizers and quarter-wave plate in the phase retardation setup. I_{dark} corresponds to possible imperfections in the polarizers or quarter-wave plate, as well as to the dark current of the photodetector. Also, the analyzer should be placed with its optical axis parallel to the polarizer, and the maximum photodetector signal, I_{max} should be measured.

2. Measurements of the parameters of the empty cell

   (1) The optical phase retardation, R_{sub}.
   (2) The capacitance (if using the YvS technique).
   (3) The gap thickness.

3. Characterization of the filled nematic cell

   (1) Determination of the pretilt angle, e.g., by the magnetic null method.[29] The possible hybridity of alignment should be verified as explained in Sec. IV B.

(2) The frequency of the applied voltage should be chosen with care. At least, it should be larger than the frequency of the Maxwell relaxation. For very high frequencies, dispersion of the dielectric permittivity tensor should be taken in account.

(3) The capacitance should be measured as a function of applied voltage. If one uses the RV technique, this measurement is not necessary.

(4) Use the Senarmont technique to determine the optical phase retardation as a function of applied voltage. This is accomplished through the measurement of the analyzer orientation (σ_{min}) which yields the minimum transmitted intensity, I_{min}. The phase retardation is related to σ_{min} through $R = 2\pi N + 2\sigma_{min}$ (where N is an integer), and the excess transmittance is given by $T_{ex} = (I_{min} - I_{dark})/(I_{max} - I_{dark})$.

The experimental results should be presented in two plots. The first plot has RCV plotted against CV or $R(V - \bar{V})$ plotted against $(V - \bar{V})$. Remember to subtract off any additional retardation which may be caused by the alignment layers. On this plot, mark the point $V_{min} = 6V_{th}$. If RCV vs CV or $R(V - \bar{V})$ vs $(V - \bar{V})$ is not monotonically decreasing at $V > V_{min}$, no reliable determination of W is possible. If the functions are monotonically decreasing for $V > V_{min}$, one can fit the data up to the voltage V_{max} defined by the 80% rule. W is then determined in a standard fashion from Eq. (14) or Eq. (21). Nevertheless, the validity of this value of W should be additionally judged by analyzing the second plot.

The second plot should have T_{ex} as a function of V. If T_{ex} is small within the voltage window (V_{min}, V_{max}) (at least $T_{ex} \lesssim 10^{-4}$), then possible in-plane inhomogeneities in the nematic cell do not affect the value of W. However, if $T_{ex} \gtrsim 10^{-3}$ and increases with V, the value of W is greatly overestimated up to the point at which $1/W$ changes from positive to negative.

VII. CONCLUSIONS

We analyzed several electric field techniques to measure the polar anchoring coefficient W of a nematic liquid crystal against polymer substrates.

In the theoretical section, we extended the original YvS model and suggested the RV technique to determine W by a simple fitting of the dependence of the optical phase retardation versus applied voltage. The RV technique preserves all the essential features of the original YvS technique but has a number of advantages, such as elimination of the necessity to pattern the electrodes and to measure the capacitance. Most importantly, the RV technique allows one to determine a local value of W (within the area of the laser beam); thus it can be used to map the anchoring coefficient as the function of the in-plane coordinates. In both techniques, the value of W should be determined only within some voltage ''window,'' the upper limit of which had not been defined unambiguously since it depends on W. We suggested a criterion of determining V_{max} without prior knowledge of W.

The central point of interest in the experimental part was the validity of the results obtained by the YvS and RV techniques. We analyzed the field dependencies of retardation and capacitance for different cells. At first sight, all the data seem to follow the familiar linear dependence when plotted in coordinates R vs $1/CV$, suggested by Yokoyama and van Sprang[12] for the fitting procedure. However, more informative are plots in the coordinates RCV vs CV or $R(V - \bar{V})$ vs $(V - \bar{V})$. These plots clearly demonstrate that the experimental behavior of many cells is quite different from that expected in the theory. Namely, the slopes of the lines RCV vs CV and $R(V - \bar{V})$ vs $(V - \bar{V})$ that are supposed to be proportional to $1/W$, are voltage dependent and can change signs. These variations are masked in the original R vs $1/CV$ presentation. The most disturbing feature of the functions RCV vs CV and $R(V - \bar{V})$ vs $(V - \bar{V})$ is that in some cells they have a positive slope (i.e., negative W) at high voltages. This behavior indicates that the optical retardation is larger than that theoretically expected for the nematic cells, even with an infinitely strong anchoring and even when all the possible non-nematic sources of phase retardation (such as retardation of the alignment layers) are taken into account. Such behavior signals that no meaningful determination of W is possible.

In-plane inhomogeneities of the cell (such as variations of the anchoring energy, easy axis, surface polarization, fractures in the patterned electrodes, etc.) are the most plausible source of the unexpected dependencies RCV vs CV and $R(V - \bar{V})$ vs $(V - \bar{V})$ as well as the unusually high values of the optical phase retardation. Our experimental measurements of the minimum light transmittance T_{ex} through the cell clearly detect voltage-dependent in-plane inhomogeneities. These inhomogeneities are not taken into account by any present theoretical model and most often lead to an overestimation of W. We suggest a protocol that allows one to verify the impact of these in-plane inhomogeneities and to check if the cell is suitable for measurements by the YvS technique or by the RV technique. An important step in this protocol is to determine how strongly the in-plane inhomogeneities modify the ''ideal'' optical response of the cell. We suggest to test this by measuring the excess transmittance. Further work might result in finding the exact relationship between T_{ex} and the excess retardation.

We also demonstrate that both YvS and RV techniques should not necessarily be applied to thick cells such as 50 μm cells; when the anchoring is strong, W can be measured for much thinner cells.

Further work, both theoretical and experimental, is definitely needed to decipher the origin and behavior of the in-plane inhomogeneities in the applied field. Theoretically, these inhomogeneities should be included while modeling the response of the cell to the applied field. Note that one should not exclude the possibility of in-plane director inhomogeneities due to pure elastic response to the applied field (even when the surface are ideally aligned and uniform). Experimentally, the possibility of in-plane components of the electric field can be examined, e.g., by comparing the behavior of cells in the electric and magnetic fields. The very procedure of measuring phase retardation with Senarmont technique in the presence of in-plane inhomogeneities of the optic axis should also be examined. Another interesting question is that about the processes (apart from dielectric

J. Appl. Phys., Vol. 86, No. 8, 15 October 1999

Nastishin *et al.* 4213

response) that the strong electric field causes within the surface region. Finally, application of the RV technique to cells where *W* changes from point to point is of great interest as well.

ACKNOWLEDGMENTS

[1] L. M. Blinov, A. Yu. Kabayenkov, and A. A. Sonin, Liq. Cryst. **5**, 645 (1989).

[2] M. Kléman and C. Williams, Philos. Mag. **28**, 275 (1973); G. Ryshenkow and M. Kléman, J. Chem. Phys. **64**, 404 (1976).

[3] G. Barbero, N. V. Madhusudana, and G. Durand, J. Phys. (France) Lett. **45**, L-613 (1984).

[4] T. Marusiy, Yu. Reznikov, and V. Reshetnyak, Sov. Phys. JETP **64**, 502 (1986).

[5] A. Rapini and M. Papoular, J. Phys. (Paris), Colloq. **30**, C-4 (1969).

[6] S. Naemura, Appl. Phys. Lett. **33**, 1 (1978).

[7] K. H. Yang and C. Rosenblatt, Appl. Phys. Lett. **43**, 62 (1983).

[8] J. T. Gleeson and P. Palffy-Muhoray, Liq. Cryst. **5**, 663 (1989).

[9] D.-F. Gu, S. Uran, and C. Rosenblatt, Liq. Cryst. **19**, 427 (1995).

[10] D. Subacius, V. M. Pergamenshchik, and O. D. Lavrentovich, Appl. Phys. Lett. **67**, 214 (1995).

[11] S. Faetti and V. Palleschi, J. Phys. (France) Lett. **45**, L-313 (1984).

[12] H. Yokoyama and H. A. van Sprang, J. Appl. Phys. **57**, 4520 (1985).

[13] H. Yokoyama, S. Kobayashi, and H. Kamei, J. Appl. Phys. **61**, 4501 (1987).

[14] H. Yokoyama, in *Handbook of Liquid Crystal Research*, edited by P. J. Collings and J. S. Patel (Oxford University Press, New York, 1997), p. 179.

[15] R. Sun and H. Yokoyama, presented at the 4th International Unit of Material Research Society International Conference in Asia, Chiba, Japan, September 1997 (unpublished).

[16] Yu. A. Nastishin, R. D. Polak, S. V. Shiyanovskii, and O. D. Lavrentovich, Appl. Phys. Lett. **75**, 202 (1999).

[17] M. I. Barnik, L. M. Blinov, T. V. Korkishko, B. A. Umansky, and V. G. Chigrinov, Mol. Cryst. Liq. Cryst. **99**, 53 (1983).

[18] O. D. Lavrentovich, V. G. Nazarenko, V. V. Sergan, and G. Durand, Phys. Rev. A **45**, R6969 (1992).

[19] G. Barbero and G. Durand, J. Appl. Phys. **67**, 2678 (1990).

[20] H. Yokoyama, Mol. Cryst. Liq. Cryst. **165**, 269 (1988).

[21] Y. Ji, J. R. Kelly, and J. L. West, Liq. Cryst. **14**, 1885 (1993).

[22] S. Stallinga, J. A. M. M. van Haaren, and J. M. A. van den Eerenbeemd, Phys. Rev. E **53**, 1701 (1996).

[23] H. J. Deuling, Mol. Cryst. Liq. Cryst. **19**, 123 (1972); L. M. Blinov and V. G. Chigrinov, *Electrooptic Effects in Liquid Crystal Materials* (Springer, New York, 1994).

[24] In their original work (see Ref. 12), Yokoyama and van Sprang state the condition as $d \gg d_E \gg d_W$, and, thus used that the thickness must be at least 100 times the anchoring extrapolation length.

[25] D.-K. Seo and S. Kobayashi, Appl. Phys. Lett. **66**, 1202 (1995); D.-K. Seo, Y. Iimura, and S. Kobayashi, *ibid.* **61**, 234 (1992).

[26] V. G. Nazarenko, A. K. St. Clair, R. Klouda, R. D. Polak, Yu. Nastishin, and O. D. Lavrentovich, Journal of the SID, 135 (1998).

[27] J.-H. Kim and C. Rosenblatt, Appl. Phys. Lett. **72**, 1917 (1998); J. Appl. Phys. **84**, 6027 (1998).

[28] M. J. Bradshaw, E. P. Raynes, J. D. Bunning, and T. E. Faber, J. Phys. (Paris) **46**, 1513 (1983).

[29] T. J. Scheffer and J. Nehring, J. Appl. Phys. **48**, 1783 (1977).

[30] M. Born and E. Wolf, *Principle of Optics* (Pergamon, Oxford, 1980); R. A. Chipman, in *Handbook of Optics II*, edited by M. Bass (McGraw–Hill, New York, 1995), Chap. 22.

[31] D. Andrienko, Y. Kurioz, Y. Reznikov, C. Rosenblatt, R. Petschek, O. Lavrentovich, and D. Subacius, J. Appl. Phys. **83**, 50 (1998); P. Ziherl, D. Subacius, A. Strigazzi, V. M. Pergamenshchik, A. L. Alexe-Ionescu, O. D. Lavrentovich, and S. Zumer, Liq. Cryst. **24**, 607 (1998).

[32] J. Nehring, A. R. Kmetz, and T. J. Sheffer, J. Appl. Phys. **47**, 850 (1976); K. H. Yang, J. Phys. (Paris) **44**, 1051 (1983).

[33] L. R. Evangelista, Phys. Lett. A **205**, 203 (1995).

[34] V. I. Sugakov and S. V. Shiyanovskii, Ukr. Phys. J. **22**, 1439 (1977).

[35] O. D. Lavrentovich and V. M. Pergamenshchik, Int. J. Mod. Phys. B **9**, 2389 (1995).